Research Article

Effects of Silane Coupling Agents on Physical Properties of Simultaneous Biaxially Stretched Polylactide Film

Suttinun Phongtamrug*
Department of Industrial Chemistry, Faculty of Applied Science, King Mongkut's University of Technology North Bangkok, Bangkok, Thailand
Integrated Chemistry Research Center for Sustainable Technology (ICRT), King Mongkut's University of Technology North Bangkok, Bangkok, Thailand

Patakorn Pilasen and Kitiya Ridthitid
Department of Industrial Chemistry, Faculty of Applied Science, King Mongkut's University of Technology North Bangkok, Bangkok, Thailand

* Corresponding author. E-mail: suttinun.p@sci.kmutnb.ac.th DOI: 10.14416/j.asep.2024.06.012
Received: 9 February 2024; Revised: 30 March 2024; Accepted: 5 April 2024; Published online: 27 June 2024

Abstract
Simultaneous biaxial stretching by using high speed was shown to improve the toughness of the polylactide (PLA) film. Additionally, a silane coupling agent was utilized to increase the mechanical strength of the product by either physical or chemical bonding. Different types of silane coupling agents influenced product properties. In this study, three types of silane coupling agents, i.e. (3-chloropropyl)trimethoxysilane (CPS), 3-aminopropyltriethoxysilane (APS), and *N*-(2-aminoethyl)-3-aminopropyltrimethoxysilane (DMS), were selected and compounded with PLA by using 0.1–2 phr. This work investigated the effects of the blended silane coupling agent on the physical properties of biaxially stretched PLA films. The blended PLA sheets were manufactured by using a chill-roll cast film extruder and the biaxially stretched films were prepared by a biaxial stretcher. An existing silane coupling agent in PLA films was confirmed by infrared spectroscopy and energy-dispersive X-ray analysis. Furthermore, thermal and tensile properties of the obtained films were determined. Flexibility of biaxially stretched PLA film with a diamino silane coupling agent was increased while its stiffness was maintained. Elongation at break of the biaxially stretched PLA film blending with DMS was increased more than 2 times. Moreover, oxygen gas permeability and water vapor permeability of the biaxially stretched PLA films with 2 phr of APS and CPS were increased compared to those of the neat one. This work provided the structural effect of coupling agents on the physical properties of biaxially stretched PLA film.

Keywords: Biaxial stretching, Bioplastic, Film, Microstructure, Polylactide, Silane coupling agent

1 Introduction

Concerning environmental issues related to plastic waste, plastic products from biodegradable polymers have been substantially substituted with petroleum-based plastics, which take hundreds of years to decompose. Biodegradable polymers have been known as materials that are utilized for a limited time before degrading under specific conditions, for example, polylactide (PLA), poly(butylene succinate) (PBS), and poly(butylene adipate-co-butylene terephthalate) (PBAT).

Compared among biodegradable polymers, PLA is one promising biodegradable polymer from bioresource, which has potential as an alternative to petroleum-based polymers. This is because of its transparency, acceptable mechanical properties, and high industrial-scale production. Moreover, to fabricate

PLA product, conventional process for commercial plastics can be adjusted and utilized. However, a main drawback of PLA is brittleness, which results from its slow crystallization rate, and it limits the product application. Up to now, there have been various approaches to improve the properties of polylactide final products, such as chemically modifying, blending with some additives, and adjusting processing conditions [1]. In this way, selecting processing technique and controlling the processing condition, such as temperature and speed, is one of the simple ways to manufacture the plastic product.

PLA has been proven to have strain-induced crystallization [2], [3]. The microstructure of the PLA has been influenced by stretching so the mechanical properties, for example, elongation, stiffness, and toughness, were improved [4]. Therefore, applying stretching force in the production process induces crystallization and, consequently, increases mechanical properties. The biaxial stretching technique is one of the techniques utilized for improving the strength and toughness of film products significantly. This technique has been applied in PP, PET and PLA. Biaxial stretching taken at a high stretching rate (> 35 mm.s^{-1}) gave the supertough PLA film with high elongation at break and toughness due to the increase in PLA crystallinity and high amount of small crystallites formed [5]. In some cases, thermoplastic starch (TPS) was blended with PLA and the films were biaxially stretched. Tensile strength and strain at break of the biaxially stretched PLA/TPS films were increased more than 4 times and 2 times, respectively, compared to those of the unstretched ones [6], [7]. Moreover, impact strength, surface hydrophobicity, and gas barrier property were markedly improved for the biaxially stretched PLA film blending with TPS and PBAT [8]. Adding a compatibilizer, which strengthens interface between PLA and PBAT, increases maximum stress before failure [9], [10]. The tear resistance of biaxially stretched PLA films was also improved after adding 5 wt% core-shell rubber [11]. Not only blending but also modifying the chemical structure are approaches to adjust the physical properties of the products obtained.

A silane coupling agent is known as one of the effective coupling agents, which is mostly used in composite materials. The chemical structure of the silane coupling agent is R′-Si-$(OR)_3$, where OR is the alkoxy group and R′ is the alkyl group containing various functional groups. The alkoxy group can be hydrolyzed to the alcohol group, then self-condensation possibly occurs and partial network structure can be obtained. The functional groups in R′, such as amine, epoxy, or chloride, possibly bond either physically or chemically with other substances. Therefore, the silane coupling agents were chosen to interact with many kinds of materials depending on both functional groups and alkoxy groups via bond linkage and intermolecular interaction. For example, amino- and isocyanate-containing silane coupling agents were hydrolyzed, condensed, and hybridized with PLA to reach supertough PLA [12]. Crosslinking of PLA was obtained by reaction with unsaturated silane coupling agents, initiated by dicumyl peroxide. This significantly increased the mechanical properties of the film obtained [13]. However, the preparation steps were quite complicated.

In our previous work, combinatorial effect of simultaneous biaxial stretching and silane coupling agent enhanced the performance of PLA film [14]. The silane coupling agent used contained one amino group (APS). However, as mentioned above, functional groups in silane coupling agents influence on properties of the product obtained. In this work, the silane coupling agent with two amino groups (DMS), which possibly form more intermolecular interaction and affect PLA film properties, was chosen. Moreover, the silane coupling agent with chloride group (CPS), which was active, was selected to mix and compare.

Simple blending with silane coupling agents has been combinatory applied with specific processing technique. The PLA was blended with some selected silane coupling agents. This blending is an uncomplicated method and feasible to upscale for manufacturing industry. Then, the PLA films were simultaneously biaxially stretched by using a high stretching speed to improve the film toughness. The physical properties of the prepared film were investigated. The relationship between the film properties and the silane coupling agent type was determined.

2 Materials and Methods

2.1 *Materials*

Polylactide (PLA) containing D-isomer 4.0% having

a relative viscosity of 4.02 (Ingeo™ Biopolymer 4043D) was bought from NatureWorks LLC. 3-Aminopropyltriethoxysilane (APS) was from Alfa Aesar. (3-Chloropropyl)trimethoxysilane (CPS) and *N*-(2-aminoethyl)-3-aminopropyltrimethoxysilane (DMS) were products of Sigma-Aldrich.

2.2 *Methods*

2.2.1 Compounding

Different types and different amounts of the silane coupling agents (0.1–2 phr) were hydrolyzed in distilled water at 30 °C for 15 min. Then, silanol compounds (0.1–2 phr) were mixed with PLA for 15 min and dried at 60 °C in a hot air oven overnight. The amount of silane coupling agents blended into PLA was labeled after the silane coupling agent type added. After drying, the mixed PLA pellets were compounded in a counter-rotating twin-screw extruder (L/D 25:1) (Thermo Electron Prism TSE 16 TC, UK) with a screw speed of 10–75 rpm. The temperatures used in the feed zone, compression zone, and fusion zone were 140–150 °C, 140–150 °C, and 145–160 °C, respectively. The extrudate was cooled by air and pelletized.

2.2.2 Sheet forming and biaxial stretching

The cast sheet was processed by a chill-roll cast film extruder (Labtech LE25-30/C and LCR-300, Thailand) with a screw (L/D 30:1) speed of 30–54 rpm. The processing temperatures and the die temperature were 150–190 °C and 160–195 °C, respectively. The thickness of the sheets was controlled to be in the range of 0.30–0.40 mm. The cast sheet was cut into 6 × 6 cm^2 and held at 95 °C for 30 s before stretching. Simultaneous biaxial stretching of the sheets was taken by a biaxial stretching machine (Ryuu, Japan) in two perpendicular directions (machine direction (MD) and transverse direction (TD)) for 5 × 5 times by using a speed of 75 mm s^{-1}. When the specified draw ratio was reached, the stretched sample was held during cooling down to room temperature. The thickness of the films after biaxial stretching was about 30–50 µm. The biaxially stretched films, i.e., biaxially oriented film, were prefixed by 'BO'.

2.3 *Characterization*

2.3.1 Structural characterization

An existing silane coupling agent in the PLA film was determined by a Fourier transform infrared (FTIR) spectrophotometer in attenuated total reflectance (ATR) mode. The samples were scanned in the range of 4,000–550 cm^{-1} with a resolution of 4 cm^{-1}. The number of the scan was set to 64.

2.3.2 Determination of thermal properties

Degradation temperature and residue at 600 °C of the sample were detected by a thermogravimetric analyzer (TGA) (Mettler Toledo TGA/DSC1, Switzerland). Under a nitrogen atmosphere, the sample was gradually heated from 40 to 700 °C by using a heating rate of 10 °C.min^{-1}.

Glass transition temperature, cold crystallization temperature, and melting temperature were determined by using differential scanning calorimetric (DSC) technique (TA Instruments DSC Q2000, USA). The sample was packed into an aluminum pan. Temperature procedure was performed as follows: heating from 20–200 °C, then cooling to 0 °C, and heating again to 200 °C. The heating and cooling procedures were done by using a rate of 10 °C min^{-1} under a nitrogen atmosphere.

Degree of crystallinity (χ_c) can be calculated in the Equation (1):

$$\chi_c\,(\%) = (\Delta H_m - \Delta H_{cc})/(f \times \Delta H_o) \times 100 \quad (1)$$

where ΔH_{cc} is cold crystallization enthalpy of the sample and ΔH_m is melting enthalpy of the sample. The ΔH_o is melting enthalpy of 100% crystalline sample. The 100% crystalline PLA showed a melting enthalpy of 93 J.g^{-1} [15]. In addition, f is weight fraction of PLA.

2.3.3 Microstructure analysis

Surface and fracture morphology of the prepared films were scanned by a scanning electron microscope (SEM) (FEI, Quanta 450). For surface analysis, the film was mounted on an aluminum stub with a conductive double-sided adhesive carbon tape. For

fracture observation, the film was immersed in liquid nitrogen. After the film was frozen, it was fractured, then the fractured part was mounted on a 90-degree angled stub. An accelerating voltage of 10 kV was applied to an electron gun for scanning. Elemental composition such as C, O, Si, Cl, and N were determined by energy-dispersive X-ray (EDX) analysis (Horiba Emax x-act).

Crystallinity of the film was checked by an X-ray diffractometer (Rigaku SmartLab, Japan) using a Cu-Kα radiation (λ = 1.5406 Å) with a Ni filter operated at 40 kV and 30 mA. X-ray diffraction (XRD) pattern was recorded in the 2θ range of 5–50° by using a scan rate of 1°.min^{-1}. A lattice spacing (d) was calculated from the reflection peak by using Bragg's law:

$$n\lambda = 2dsin\ \theta \quad (2)$$

where n is integer. A crystallite size (D) was calculated by Scherrer equation,

$$D = K\lambda/\beta cos\ \theta \quad (3)$$

where K and β are shape factors and full width at half maximum of the selected peak, respectively.

2.3.4 Mechanical testing

Mechanical properties, i.e., tensile strength, Young's modulus, and elongation at break, of the films were carried out by using a universal testing machine (Instron 55R1123, USA) in a tensile mode with a 500 N load cell. The film samples were cut into the specified shape and the prepared samples were drawn with a crosshead speed of 5 mm.s^{-1} according to ASTM D882-18. The films in both machine direction (MD) and transverse direction (TD) were tested. Each sample was measured in quintuplicate.

2.3.5 Gas permeability measurement

Oxygen transmission rate (OTR) of the prepared film was tested according to GB/T 1038–2000 by a gas permeability tester (Labthink PERME VAC-V2). The films were cut into circles with a diameter of 10 cm. Differential pressure method was carried out at 23 ± 2 °C and 50–70% relative humidity. The chamber was vacuumed before applying an oxygen flow rate of 100 mL.min^{-1}.

Water vapor transmission rate (WVTR) of the prepared film was performed following ASTM E398-13 by using a water vapor permeability testing machine (Mocon Permatran-W398). The measurements were carried out at 38 °C and 90% relative humidity by using nitrogen gas with a flow rate of 250 mm.min^{-1} as a carrier gas. Water vapor permeability coefficient (WVP) was calculated from multiplication of water vapor transmission rate (WVTR) and thickness of the film.

2.3.6 Testing of film shrinkage

A shrinkage of the stretched film was tested following ASTM D2732-03. The film was cut into 10 × 10 cm^2. The initial length (L_0) was recorded in two decimal places. The film was soaked in a hot oil bath at 100 °C for 15 s, then the film was put into cold water and dried. The length of the film after soaking in the oil bath (L) was measured and compared with the initial length (L_0). The average thermal shrinkage was calculated from triplicate samples.

$$\%\ Shrinkage = (L_0 - L)/L_0 \times 100 \quad (4)$$

3 Results and Discussion

3.1 *Confirmation of silane coupling agents in PLA*

An evidence of existing silane coupling agent in the sample was checked by TGA. PLA showed a one-step decomposition with an onset degradation temperature of 340 °C. The PLA blended with silane coupling agents, either CPS, APS, or DMS, also showed a one-step decomposition. However, the onset degradation temperatures of PLA with any types of silane coupling agent were lower than that of PLA. This might be due to existence of alkyl short chain and different atoms, such as chlorine in CPS and nitrogen in APS and DMS. The one containing high number of amino groups and long alkyl chain, i.e. DMS, lowered the onset degradation temperature to 326 °C. Moreover, the residues at 500 °C of the PLA films blended with 2 phr of any silane coupling agents were higher that of PLA about 3–4%. This increasing residue obviously came from the remaining Si and C of the silane coupling agent in the PLA film.

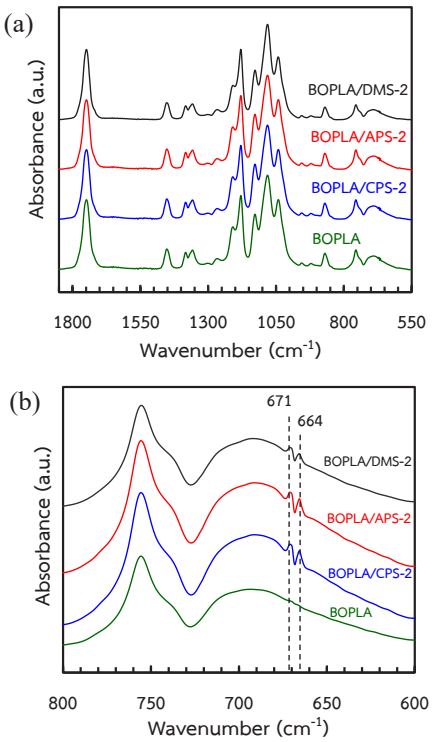

Figure 1: FTIR spectra of the BOPLA film and the BOPLA films with CPS, APS, and DMS at 2 phr in the range of (a) 1850–550 cm^{-1} and (b) 800–600 cm^{-1}.

To investigate feasibility of a chemical reaction between silane coupling agents and PLA, FTIR spectroscopic technique was performed. Figure 1 shows FTIR spectra of biaxially stretched PLA films without and with 2 phr of silane coupling agents. The pure BOPLA film shows some significant peaks at 1750, 1180, and 1083 cm^{-1}, relating to C=O stretching, C-O-C asymmetry stretching, and C-O-C symmetry stretching, respectively [16]. After blending with silane coupling agents, either APS, CPS, or DMS, new fermi doublet peaks at 671 and 664 cm^{-1} appeared. These peaks, corresponding to Si-O deformation [17], confirmed an existence of silane coupling agent in the PLA films. Although the formations of Si-O-Si groups have been reported to show the peaks at 1130–1000 cm^{-1} [18], these peaks are not clearly observed due to overlapping with C-O-C stretching peaks in PLA. However, it should be noted that, in case that grafting or crosslinking possibly occurred, glass transition temperatures of the obtained films might be increased (Table 1).

Table 1: Onset glass transition temperature (T_g), cold crystallization temperature (T_{cc}), melting temperature (T_m), and degree of crystallinity (χ_c) of the biaxially stretched films (from the second heating scan)

Sample	T_g (°C)	T_{cc} (°C)	T_m (°C)	χ_c (%)
BOPLA	57.0	121.8	150.7	25.3
BOPLA/CPS 0.1	57.3	119.0	150.2	28.6
BOPLA/CPS 0.5	57.4	117.1	149.7, 154.9	27.2
BOPLA/CPS 1	57.6	110.0	148.3, 154.0	31.2
BOPLA/CPS 2	57.7	113.9	149.0, 154.4	34.7
BOPLA/APS 0.1	57.5	119.7	150.1	25.6
BOPLA/APS 0.5	57.9	119.8	150.2, 156.6	30.3
BOPLA/APS 1	58.0	114.1	149.8, 156.6	29.2
BOPLA/APS 2	58.2	117.3	150.3, 156.8	29.7
BOPLA/DMS 0.1	57.2	121.7	150.6	25.9
BOPLA/DMS 0.5	57.4	120.2	150.7	34.5
BOPLA/DMS 1	57.7	120.4	150.8	31.5
BOPLA/DMS 2	57.4	115.4	148.0, 154.1	36.4

The existence of silane coupling agents in the PLA films was confirmed by SEM-EDX analysis. Figure 2 shows surface and fracture morphology of the prepared films obtained by SEM and elemental composition determined by EDX. The surface morphology of the films was smooth except some creases appeared in the one with CPS. All films gave similar fracture morphology without large cavity. Considering EDX results, the C and O signals were observed in the BOPLA film. In addition, the Si signals were detected in all blended BOPLA films. Furthermore, the N signals were found in the films containing APS and DMS, whereas the Cl signal was shown in the film blended with CPS. These findings supported the remaining Si in the prepared films.

3.2 *Effect of silane coupling agent type on thermal properties of the PLA films*

Since simultaneous biaxial stretching at high speed was known to improve mechanical properties of the PLA film, those properties were related to the film crystallinity [5]. Changes in crystallinity degree and thermal properties of the biaxially stretched films were traced by DSC. The influence of the silane coupling agents on PLA was investigated from the second heating scans, which removed thermal history from processing

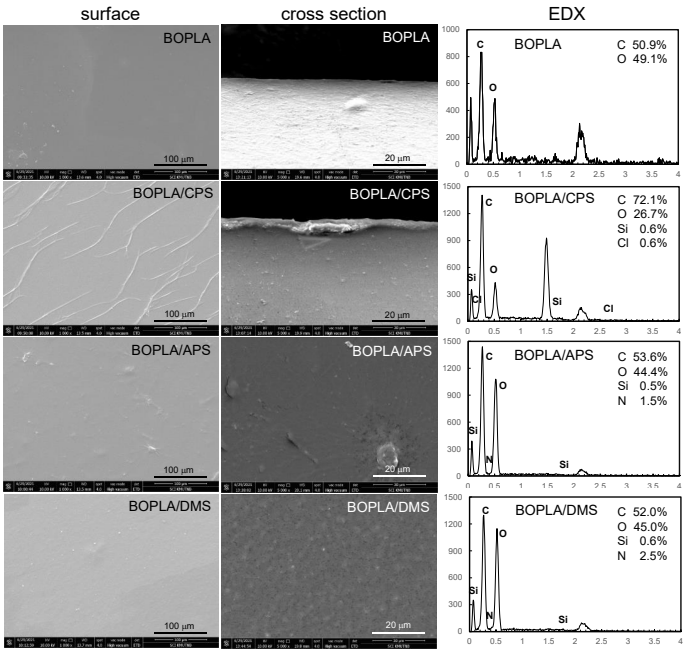

Figure 2: Surface and fracture morphology of biaxially stretched PLA films without and with silane coupling agents 2 phr by SEM and elemental composition of surface morphology from EDX analysis.

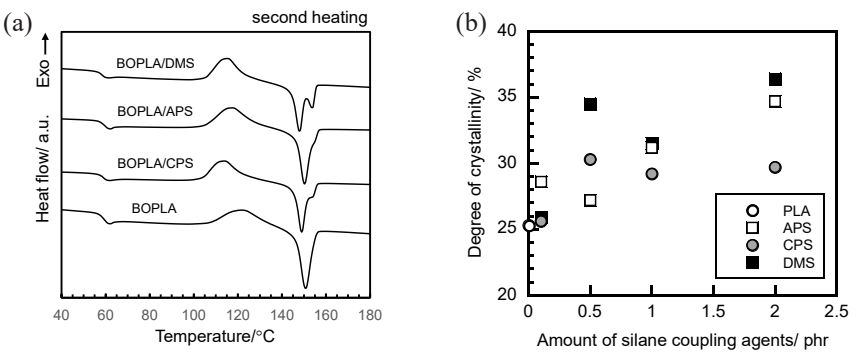

Figure 3: (a) DSC thermograms from second heating scans of the BOPLA film and the BOPLA films with CPS, APS, and DMS at 2 phr. (b) Crystallinity degree of the BOPLA with different types and amounts of treated silane coupling agent.

(Figure 3(a)). The BOPLA showed an onset glass transition temperature (T_g), a cold crystallization temperature (T_{cc}), and a melting temperature (T_m) at 57, 121.8, and 150.7 °C, respectively. The blending with silane coupling agents affected the glass transition temperature of the films. As shown in Table 1, T_gs of all blended PLA films were shifted from that of the BOPLA film, which might be due to chain entanglement.

However, the cold crystallization temperature was reduced, i.e., the PLA crystallization was enhanced by the heterogeneous nucleation as found in many cases [19]–[21]. This also affected the crystallinity fraction of the blended films. Crystallinity degree of the film was increased from 25.3–36.4% after adding silane coupling agents (Figure 3(b)).

Considering the melting region, the PLA film showed one T_m at 150.7 °C, referring to a α′ (disorder α) phase [22]–[24]. Addition of silane coupling agents

induced, not only the crystallinity fraction [25], but also formation of both α′ and α phases, as observed from two melting points. This showed that the addition of the silane coupling agents feasibly formed the order crystalline phase. The formation of α phase also confirmed the strengthened film after silanization [26].

Degree of crystallinity calculated from DSC of the biaxially stretched PLA film is 25.3%. Adding some amount of silane coupling agents improved the crystallinity fraction in PLA film. The degree of crystallinity was increased up to 36.4% in the case of adding 2 phr DMS. The reason that the silane coupling agents improve crystallinity degree of PLA can be explained by heterogeneous nucleation [27], [28]. That is to say, nucleation was promoted by a foreign compound, which acted as nucleation sites, similar to the addition of impurities in the system, then crystallization was accelerated. Considering the amount of coupling agents added, the variation of crystallinity degree values obtained was observed. This possibly came from nonuniform dispersion of silane coupling agents. However, the results showed an increasing trend for blending all types of silane coupling agents into PLA. As shown in Table 1, the BOPLA/DMS 2 film gave the highest degree of crystallinity. This might be explained by the DMS structure, containing two amino groups and a long alkyl chain, which induced chain arrangement by intermolecular interaction.

3.3 *Mechanical properties of the prepared film*

Tensile strengths of the BOPLA film in MD direction and TD direction were found to be 74.4 ± 7.3 MPa and 64.1 ± 4.3 MPa, respectively. Young's moduli of the BOPLA film were 2.8 ± 0.4 GPa and 2.7 ± 0.1 GPa in MD and TD directions, respectively. In addition, elongation at break of the BOPLA film in MD and TD direction were 12.6 ± 2.8% and 10.8 ± 1.6%, respectively. These data indicated that the strength and toughness of the BOPLA film in MD direction were higher than those in TD direction, although there were not much difference.

Effect of type and content of silane coupling agents on mechanical properties of the BOPLA films were investigated. Figure 4 shows tensile strength, Young's moduli, and elongation at break of the prepared films. Blending with CPS hardly affected tensile strength and Young's moduli of the films but it somehow increased elongation of the films. Some fluctuation of the obtained values might possibly come from inhomogenous blending. Although CPS blending induced the PLA crystallinity and formation of α-form crystal, the strength of biaxially stretched films was maintained. This showed that CPS was also in amorphous phase, which increased plasticity of the sample.

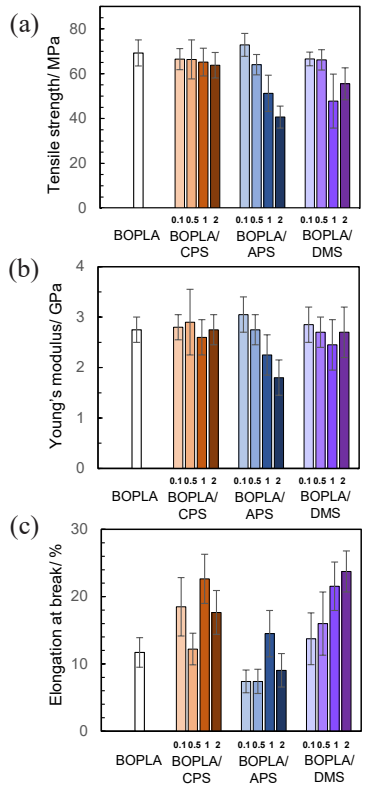

Figure 4: (a) Tensile strength, (b) Young's moduli, and (c) elongation at break of the biaxially stretched films.

In the case of BOPLA/APS, both tensile strength and Young's moduli of the films decreased with increasing amount of APS. Elongation at break of the BOPLA/APS films also decreased when comparing with the BOPLA films, except the BOPLA blended with APS 1 phr. The decreasing tensile properties of the prepared films might be related to an occurrence of small-sized voids during biaxial stretching at high speed [29], [30]. This situation was feasibly occurred in all biaxially stretched films.

The effect of increasing number of amino groups and chain lengths of silane coupling agents on mechanical strength of the products were already proposed [31], [32]. However, from the best of our knowledge, there have been no reported for the biaxially stretched film. Addition of DMS significantly improved elongation at break but slightly decreased tensile strength and moduli of the biaxially stretched PLA films. This showed that, not only high amount of small crystallite from high-speed biaxial stretching [5], but the intermolecular interaction, i.e. hydrogen bond, created by amino groups and carboxyl groups in PLA also improved the film flexibility.

Comparing APS and DMS blending, both compounds contain amino groups but the higher amount of amino groups (DMS) results in higher intermolecular interactions. This was evident by increased elongation at break of the BOPLA/DMS films. The results of tensile properties can be summarized that combination of the biaxial stretching and the blended DMS maintain stiffness and clearly improve toughness of PLA.

3.4 *Microstructure analysis of the biaxially stretched film*

Simultaneous biaxial stretching has been proposed as the technique to induce crystallinity of the polymer films, resulting in high strength and toughness. The crystallinity was significantly increased as confirmed by DSC and XRD. To examine the influence of silane coupling agents in the PLA film, X-ray diffraction measurements were performed. Figure 5(a) compares the XRD patterns of the BOPLA films with that of PLA sheet. All biaxially stretched films showed a sharp diffraction peak at 16.4°, corresponding to (110)/(200) reflection planes of α (or disorder α) phase [33], [34], while the PLA sheet gave a broad band, relating to amorphous sample. Figure 5(b) plots crystallite size and lattice spacing of the biaxially stretched films. Blending APS and DMS into the PLA films reduced the (110)/(200) lattice spacing of PLA from 5.43 Å to 5.39 Å. This lattice spacing corresponded to an *a*-axis of PLA crystal structure, which was a distance between two polymer chains. However, the crystallite size of PLA was significantly increased from 5.76 nm to 6.52 nm (13.2%), 7.15 nm (24.1%), and 9.42 nm (63.5%) for CPS, APS, and DMS, respectively. This implied that the added silane coupling agent, especially

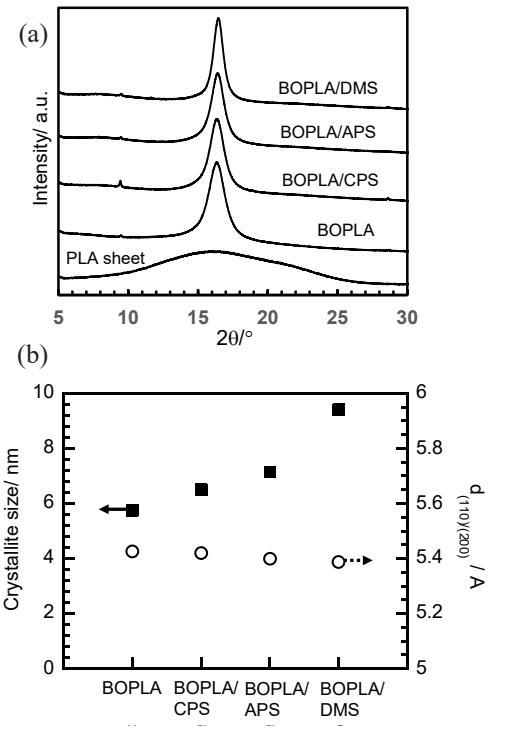

Figure 5: (a) XRD patterns of PLA with silane coupling agents 2 phr and (b) crystallite size and lattice spacing of the biaxially stretched PLA films.

the one containing amino group, might be excluded from the crystal structure of PLA, as seen in an *a*-axis contraction of the PLA crystal structure. Meanwhile, it induced arrangement of nanoscale crystallite microstructure. As the results shown, the DMS, containing long alkyl chain and two amino groups, clearly induced crystallite formation. Considering the relationship between crystallite size and crystallinity degree of the blended biaxially stretched film, the increasing crystallite size related to the increasing crystallinity degree of PLA observed by DSC.

3.5 *Gas Barrier of the biaxially stretched film*

Gas barrier is one of important properties to be considered for packaging materials. The PLA film has been reported to show a moderate oxygen barrier [35], [36]. The crystallinity plays an important role in gas barrier, i.e., a high crystalline or order-structured film significantly decreased gas permeability, compared to an amorphous film [37], [38]. Therefore, gas

barrier of the biaxially stretched film, which has high crystallinity, is higher than the unstretched film. With the same stretching condition, the gas barrier properties of the obtained films depend on the type of silane coupling agents added. Table 2 shows oxygen permeability coefficients and water vapor permeability coefficients of BOPLA and the biaxially stretched PLA films containing silane coupling agents at 2 phr.

Oxygen permeability coefficient of the prepared BOPLA film is $2.7 \pm 0.2 \times 10^{-14}$ $cm^3.cm.cm^{-2}.s^{-1}.Pa^{-1}$. Blending with APS and DMS hardly affects the oxygen permeability coefficient of the films. However, the blending with CPS increased the oxygen permeability coefficient of the films by more than 50% for CPS 2 phr. This might come from some spaces or voids generated by repulsive force from chlorine atoms although the crystallinity degree of the BOPLA/CPS was higher than that of BOPLA film.

Considering water vapor barrier properties, addition of silane coupling agents increased the water vapor permeability coefficient of the prepared films. In other words, the water vapor barrier of BOPLA film declined after blending with any coupling agents. This was possibly explained by formation of voids in microstructure of the prepared film. Furthermore, water vapor permeation depends on intermolecular interaction with the chemical structure in the film such as hydrogen bonds. In this way, a balance between formed voids and intermolecular interaction from blended substances manipulated the water vapor permeability coefficient of the films.

Table 2: Oxygen permeability coefficients and water vapor permeability coefficients of BOPLA and the biaxially stretched PLA films containing different types of silane coupling agents at 2 phr

Sample	Oxygen Permeability Coefficient ($\times 10^{-14}$ $cm^3.cm.cm^{-2}.s^{-1}.Pa^{-1}$)	Water Vapor Permeability Coefficient ($g.mil.m^{-2}.d^{-1}$)
BOPLA	2.7 ± 0.2	84.2 ± 12.8
BOPLA/CPS 2	4.2 ± 0.6	104.7 ± 9.4
BOPLA/APS 2	3.0 ± 0.5	168.7 ± 2.5
BOPLA/DMS 2	2.6 ± 0.5	98.5 ± 6.4

3.6 *Thermal shrinkage of the prepared film*

Stretching the film produced the internal residual stress remaining in the film. When the stretched film was re-heated, the film was shrunk at a certain value and covered the products. The shrinkage of the film is about 30–50% depending on its application. The film with high shrinkage has an advantage in utilizing a low quantity of raw materials. Thermal shrinkage of the films was carried out at 100 °C.

The BOPLA film was thermally shrunk at 40.9 ± 4.5%. This corresponded to residue internal stress from high-speed simultaneous biaxial stretching of the precursor sheets. Similar shrinkage was observed in both MD and TD directions, implying the isotropic cast sheets. Addition of silane coupling agents also influenced on thermal shrinkage of the biaxially stretched films. Thermal shrinkage of the BOPLA/CPS 2, BOPLA/APS 2, and BOPLA/DMS 2 films were 33.7 ± 1.5%, 33.0 ± 4.7%, and 20.0 ± 6.0%, respectively. The decreased thermal shrinkage after blending with any silane coupling agents indicated the consequence of silane coupling agents on releasing internal stress from stretching. Due to intermolecular interaction and chain mobility, the DMS molecules, having two amino groups and long chain length, retain the microstructure of biaxially stretched PLA film, hence, the BOPLA/DMS films gave the least thermal shrinkage.

4 Conclusions

Biaxial stretching technique has been utilized to produce a tough plastic film in an industrial scale. This technique can be applied to PLA, which is originally brittle. To facilitate industrial development, blending with a coupling agent is the simplest method. Three types of silane coupling agents (CPS, APS, and DMS) were blended into PLA and simultaneous biaxial stretching of the films was carried out (Figure 6). With the same stretching condition, blending with DMS 2 phr into PLA improved toughness and maintained elastic strength of the biaxially stretched PLA films. This was caused by intermolecular interaction formed among amino groups, ester groups, and hydroxyl groups, especially in an amorphous phase. Furthermore, DMS addition kept the shape of the biaxially stretched films after thermal shrinkage testing. For application of oxygen gas permeable film, addition of CPS 2 phr was suitable while blending of APS 2 phr was applicable for preparing water vapor permeable film.

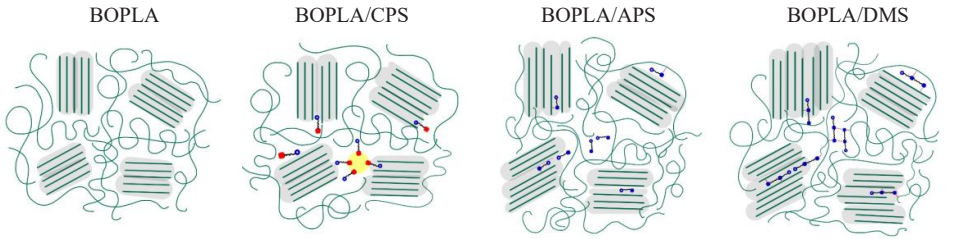

Figure 6: Schematic draw of BOPLA, BOPLA/CPS, BOPLA/APS, and BOPLA/DMS films.

Acknowledgments

The authors sincerely appreciated Prof. Suwabun Chirachanchai (Chulalongkorn University, Thailand) for providing a biaxial stretching machine. This research was partially funded by Faculty of Applied Science, King Mongkut's University of Technology North Bangkok, Thailand (contract no. 663138).

Author Contributions

S.P.: conceptualization, research design, investigation, methodology, data curation, data analysis, writing an original draft, reviewing and editing, funding acquisition, project administration; P.P. and K.R.: investigation, data curation, data analysis. All authors have read and agreed to the published version of the manuscript.

Conflicts of Interest

The authors declare no conflict of interest.

References

[1] L. T. Lim, R. Auras, and M. Rubino, "Processing technologies for poly(lactic acid)," *Progress in Polymer Science*, vol. 33, no. 8, pp. 820–852, 2008.

[2] C. Zhou, H. Li, W. Zhang, J. Li, S. Huang, Y. Meng, J. de Claville Christiansen, D. Yu, Z. Wu, and S. Jiang, "Thermal strain-induced cold crystallization of amorphous poly(lactic acid)," *CrystEngComm*, vol. 18, no. 18, pp. 3237–3246, 2016.

[3] C. Zhou, H. Li, W. Zhang, J. Li, S. Huang, Y. Meng, J. de Claville Christiansen, D. Yu, Z. Wu, and S. Jiang, "Direct investigations on strain-induced cold crystallization behavior and structure evolutions in amorphous poly(lactic acid) with SAXS and WAXS measurements," *Polymer*, vol. 90, pp. 111–121, 2016.

[4] J. Takagi, T. Nemoto, T. Takahashi, T. Taniguchi, and K. Koyama, "Improvement of mechanical properties for poly(L-lactic acid) film through drawing process optimization," *Fiber*, vol. 60, no. 7, pp. 230–234, 2004.

[5] P. Jariyasakoolroj, K. Tashiro, H. Wang, H. Yamamoto, W. Chinsirikul, N. Kerddonfag, and S. Chirachanchai, "Isotropically small crystalline lamellae induced by high biaxial-stretching rate as a key microstructure for super-tough polylactide film," *Polymer*, vol. 68, pp. 234–245, 2015.

[6] P. Jariyasakoolroj, K. Tashiro, W. Chinsirikul, N. Kerddonfag, and S. Chirachanchai, "Microstructural analyses of biaxially oriented polylactide/modified thermoplastic starch film with drastic improvement in toughness," *Macromolecular Materials and Engineering*, vol. 304, no. 9, 2019, Art. no. 1900340.

[7] P. Jariyasakoolroj, R. Supthanyakul, A. Laobuthee, A. Lertworasirikul, R. Yoksan, S. Phongtamrug, and S. Chirachanchai, "Structure and properties of in situ reactive blend of polylactide and thermoplastic starch," *International Journal of Biological Macromolecules*, vol. 182, pp. 1238–1247, 2021.

[8] R. Yoksan, K. M. Dang, A. Boontanimitr, and S. Chirachanchai, "Relationship between microstructure and performances of simultaneous biaxially stretched films based on thermoplastic starch and biodegradable polyesters," *International Journal of Biological Macromolecules*, vol. 190, pp. 141–150, 2021.

[9] R. Al-Itry, K. Lamnawar, A. Maazouz, N. Billon, and C. Combeaud, "Effect of the simultaneous

biaxial stretching on the structural and mechanical properties of PLA, PBAT and their blends at rubbery state," *European Polymer Journal*, vol. 65, pp. 288–301, 2015.

[10] N. Jaouadi, R. Al-Itry, A. Maazouz, and K. Lamnawar, "Biaxial orientation of PLA/PBAT/thermoplastic cereal flour sheets: Structure-processing-property relationships," *Polymers*, vol. 15, no. 9, 2023, Art. no. 2068.

[11] L. Boonthamjinda, N. Petchwatana, S. Covavisaruch, W. Chinsirikul, and N. Kerddonfag, "Biaxially-stretched poly(lactic acid) (PLA) and rubber-toughened PLA films: tensile and physical properties," *Key Engineering Materials*, vol. 659, pp. 363–367, 2015.

[12] X. Meng, N. A. Nguyen, H. Tekinalp, E. Lara-Curzio, and S. Ozcan, "Supertough PLA-silane nanohybrids by in situ condensation and grafting," *ACS Sustainable Chemistry & Engineering*, vol. 6, no. 1, pp. 1289–1298, 2018.

[13] C. Han, J. Bian, H. Liu, L. Han, S. Wang, L. Dong, and S. Chen, "An investigation of the effect of silane water-crosslinking on the properties of poly(L-lactide)," *Polymer International*, vol. 59, no. 5, pp. 695–703, 2010.

[14] S. Phongtamrug, R. Makhon, and T. Wiriyosuttikul, "Enhanced performance of polylactide film via simultaneous biaxial stretching and silane coupling agent as a thermal shrinkable film," *Applied Science and Engineering Progress*, vol. 16, no. 2, 2023, doi: 10.14416/j.asep.2022.02.008, Art. no. 5699.

[15] E. W. Fischer, H. J. Sterzel, and G. Wegner, "Investigation of the structure of solution grown crystals of lactide copolymers by means of chemical reactions," *Kolloid-Zeitschrift und Zeitschrift für Polymere*, vol. 251, no. 11, pp. 980–990, 1973.

[16] G. Kister, G. Cassanas, M. Vert, B. Pauvert, and A. Térol, "Vibrational analysis of poly(L-lactic acid)," *Journal of Raman Spectroscopy*, vol. 26, no. 4, pp. 307–311, 1995.

[17] K. Bukka, J. D. Miller, and J. Shabtai, "FTIR study of deuterated montmorillonites: Structural features relevant to pillared clay stability," *Clays and Clay Minerals*, vol. 40, no. 1, pp. 92–102, 1992.

[18] P. J. Launer, "Infrared analysis of organosilicon compounds: Spectra-structure correlations," in *Silicon Compounds: Silanes & Silicones*, 3rd ed., B. Arkles, Ed. Pennsylvania: Gelest Inc, pp. 175–178, 2013.

[19] H. Li and M. A. Huneault, "Effect of nucleation and plasticization on the crystallization of poly(lactic acid)," *Polymer*, vol. 48, no. 23, pp. 6855–6866, 2007.

[20] J. Nomai, B. Suksut, and A. K. Schlarb, "Crystallization behavior of poly(lactic acid)/titanium dioxide nanocomposites," *KMUTNB International Journal of Applied Science and Technology*, vol. 8. No. 4, pp. 251–258, 2015.

[21] T. Ageyeva, J. G. Kovács, and T. Tábi, "Comparison of the efficiency of the most effective heterogeneous nucleating agents for poly(lactic acid)," *Journal of Thermal and Analysis and Calorimetry*, vol. 147, pp. 8199–8211, 2022.

[22] M. L. Di Lorenzo, "Calorimetric analysis of the multiple melting behavior of poly(L-lactic acid)," *Journal of Applied Polymer Science*, vol. 100, no. 4, pp. 3145–3151, 2006.

[23] M. L. Di Lorenzo and R. Androsch, "Melting of α′- and α-crystals of poly(lactic acid)," *AIP Conference Proceedings*, vol. 1736, no. 1, 2016, Art. no. 020009.

[24] M. C. Righetti, M. Gazzano, M. L. Di Lorenzo, and R. Androsch, "Enthalpy of melting of α′- and α-crystals of poly(l-lactic acid)," *European Polymer Journal*, vol. 70, pp. 215–220, 2015.

[25] R. Bouza, A. Lasagabaster, M. J. Abad, and L. Barral, "Effects of vinyltrimethoxy silane on thermal properties and dynamic mechanical properties of polypropylene–wood flour composites," *Journal of Applied Polymer Science*, vol. 109, no. 2, pp. 1197–1204, 2008.

[26] A. J. Müller, M. Ávila, G. Saenz, and J. Salazar, "Chapter 3-Crystallization of PLA-based Materials," in *Poly(lactic acid) Science and Technology: Processing, Properties, Additives and Applications*. London, UK: Royal Society of Chemistry, pp. 66–98, 2015.

[27] M. Yang, J. Su, Y. Zheng, C. Fang, W. Lei, and L. Li, "Effect of different silane coupling agents on properties of waste corrugated paper fiber/polylactic acid composites," *Polymers*, vol. 15, 2023, Art. no. 3525.

[28] M. A. Ortenzi, L. Basilissi, H. Farina, G. D. Silvestro, L. Piergiovanni, and E. Mascheroni, "Evaluation of crystallinity and gas barrier properties of films obtained from PLA nanocomposites synthesized via in situ polymerization of L-lactide with silane-modified nanosilica and montmorillonite," *European Polymer Journal*, vol. 66, pp. 478–491, 2015.

[29] C. C. Chu and A. Needleman, "Void nucleation effects in biaxially stretched sheets," *Journal of Engineering Materials and Technology*, vol. 102, pp. 249–256, 1980.

[30] W. Fang, G. Liang, J. Li, and S. Guo, "Microporous formation mechanism of biaxial stretching PA6/PP membranes with high porosity and uniform pore size distribution," *Polymers*, vol. 14, 2022, Art. no. 2291.

[31] K. Chen, P. Li, X. Li, C. Liao, X. Li, and Y. Zuo, "Effect of silane coupling agent on compatibility interface and properties of wheat straw/polylactic acid composites," *International Journal of Biological Macromolecules*, vol. 182, pp. 2108–2116, 2021.

[32] S. Yu, K. H. Oh, J. Y. Hwang, and S. H. Hong, "The effect of amino-silane coupling agents having different molecular structures on the mechanical properties of basalt fiber-reinforced polyamide 6,6 composites," *Composites Part B*, vol. 163, pp. 511–521, 2019.

[33] J. Zhang, K. Tashiro, H. Tsuji, and A. J. Domb, "Disorder-to-order phase transition and multiple melting behavior of poly(L-lactide) investigated by simultaneous measurements of WAXD and DSC," *Macromolecules*, vol. 41, pp. 1352–1357, 2008.

[34] J. Zhang, Y. Duan, H. Sato, H. Tsuji, I. Noda, S. Yan, and Y. Ozaki, "Crystal modifications and thermal behavior of poly(L-lactic acid) revealed by infrared spectroscopy," *Macromolecules*, vol. 38, pp. 8012–8021, 2005.

[35] X. Z. Tang, P. Kumar, S. Alavi, and K. P. Sandeep, "Recent advances in biopolymers and biopolymer-based nanocomposites for food packaging materials," *Critical Reviews in Food Science and Nutrition*, vol. 52, pp. 426–442, 2012.

[36] S. Marano, E. Laudadio, C. Minnelli, and P. Stipa, "Tailoring the barrier properties of PLA: A state-of-the-art review for food packaging applications," *Polymers*, vol. 14, no. 8, 2022, Art. no. 1626.

[37] A. Guinault, C. Sollogoub, S. Domenek, A. Grandmontagne, and V. Ducruet, "Influence of crystallinity on gas barrier and mechanical properties of PLA food packaging films," *International Journal of Material Forming*, vol. 3, pp. 603–606, 2010.

[38] S. Sato, T. Nyuui, G. Matsuba, and K. Nagai, "Correlation between interlamellar amorphous structure and gas permeability in poly(lactic acid) films," *Journal of Applied Polymer Science*, vol. 131, 2014, Art. no. 40626.